

## Towards Large Scale Production of CNF for Catalytic Applications

I. KVANDE, Z. YU, T. ZHAO, M. RÖNNING, A. HOLMEN and D. CHEN

Department of Chemical Engineering, Norwegian University of Science and Technology, NTNU, N-7491 Trondheim (Norway)

E-mail: chen@chemeng.ntnu.no

### Abstract

A systematic investigation of carbon nanotubes (CNT) and nanofibre (CNF) growth in terms of structures of carbon nanomaterials and growth rates by chemical vapour deposition is summarized. Different catalysts such as unsupported  $\text{Fe}_3\text{O}_4$  and supported Ni, Fe and NiFe catalysts and different carbon sources such as CO,  $\text{CO}/\text{H}_2$ ,  $\text{CH}_4/\text{H}_2$ ,  $\text{C}_2\text{H}_6/\text{H}_2$  and  $\text{C}_2\text{H}_4/\text{CO}/\text{H}_2$  have been applied. This short review has been addressed to identify the principles for controlled synthesis of carbon nanotube or nanofibre with well-defined structures. The production of relatively high yields of defined structures is obtained. The Ni catalyst produces almost exclusively fishbone CNFs, while the supported Fe catalyst produces multiwall CNTs (MWCNTs). The NiFe catalyst can give a structure intermediate of the two. Unsupported  $\text{Fe}_3\text{O}_4$  results in the platelet structure. The diameter of the produced structures holds information on the growth mechanism. The diameters of the MWNTs are always smaller than the growth catalyst particles, while the fishbone CNFs always have larger diameter than the growth catalyst. The structure and growth rate reflect the different reactivity of the metals and the dependence on surface orientation of the catalyst particles. Higher temperature and lower partial pressure yield smaller diameter MWNTs with fewer walls and a larger inner hollow core. The space velocity and thereby the  $\text{H}_2$  partial pressure in the reactor has been identified as the most important parameter for scale-up of the reactor.

### INTRODUCTION

Carbon nanofibres (CNF) and Carbon nanotubes (CNT) have recently gained much interest for a series of applications due to their unique properties [1]. In particular, the inertness, the presence of stabilizing surface groups, and the conductivity and mesoporous character are thought to be interesting in terms of heterogeneous catalysis and electrocatalysis.

CNF and CNT have been applied as catalysts and catalyst supports. The CNFs with the graphitic sheet orientation having an angle of 0 (carbon nanotube), 20–45 (fishbone) and 90 (platelet) with respect to the fibre axis are typical structures. It has been found that the orientation of the graphitic sheet in CNF has significant effects on the properties of supported metal particles [2]. This has stimulated the research on controlled synthesis of CNF with well-defined structures. Moreover, the

commercialization and use of CNFs relies on improving the synthesis process aiming at reducing the production costs and controlling the quality. In this respect, the effect of parameters like metal catalyst, gas precursor, hydrogen partial pressure, temperature and reactor design have been studied in the synthesis of differently structured carbon nanomaterials. Fishbone CNFs are most often synthesized on supported Ni catalysts. Typically, MWNTs are obtained at higher temperatures (700–1000 °C), while CNFs are obtained at lower temperatures (400–700 °C). Hydrogen is considered important both to inhibit polymerization and encapsulation of the metal and to saturate the dangling bonds of graphite for preparing certain nanostructures [3]. This article reviews the work done in our laboratory in controlled synthesis of CNFs, where the role of metal, precursor gas, temperature and residence time is presented and discussed. The

TABLE 1

Structure, diameter and yield obtained for unsupported Fe<sub>3</sub>O<sub>4</sub> and supported Ni, Fe and NiFe (1 : 1) for CO, CO/H<sub>2</sub>, CH<sub>4</sub>/H<sub>2</sub>, C<sub>2</sub>H<sub>6</sub>/H<sub>2</sub>, and C<sub>2</sub>H<sub>4</sub>/CO/H<sub>2</sub>

Catalyst	Fe <sub>3</sub> O <sub>4</sub> ,			Fe-HT (76.7 mass % Fe),			Ni-HT (77.5 mass % Ni),			Ni : Fe = 1 : 1/Al <sub>2</sub> O <sub>3</sub> (20 mass % total),		
	$d_p = 50 \text{ nm}^a$ [4]			$d_p = 28 \text{ nm}^a$ [4, 6]			$d_p = 16 \text{ nm}^b$ [5, 6]			$d_p = 28 \text{ nm}^a$ [7, 8]		
	Structure	$d_c$ , nm	Growth rate, g C/(g cat. h)	Structure	$d_c$ , nm	Growth rate, g C/(g cat. h)	Structure	$d_c$ , nm	Growth rate, g C/(g cat. h)	Structure	$d_c$ , nm	Growth rate, g C/(g cat. h)
CH <sub>4</sub> <sup>c</sup>	Onion, MWNT	22 <sup>d</sup>	—	MWNT, Onion	13	0.176	FB	35	1.15	FB-Tubular	31	0.27
C <sub>2</sub> H <sub>6</sub> /H <sub>2</sub> 30 : 50 ml/min	MWNT, F-T	21	0.053	MWNT, FB- Tubular	19	0.264	—	—	—	—	—	—
C <sub>2</sub> H <sub>4</sub> /H <sub>2</sub> 40 : 10 ml/min	—	—	—	Tar	—	—	FB	38	9.40	—	—	—
C <sub>2</sub> H <sub>4</sub> /CO/H <sub>2</sub> 40 : 10 : 10 ml/min	—	—	—	Disordered	24	5.5	FB	33	8.00	—	—	—
CO/H <sub>2</sub> 40 : 10 ml/min	Platelet	116	3.39	FB- Tubular	45	2.07	Bamboo- FB	34	1.37	MWNT, CNF	22	0.64
CO	Onion, MWNT	32 <sup>d</sup>	—	Onion, MWNT	27	0.275	—	—	—	MWNT	~15	0.22

Note. Underlined structures are dominating in the sample. Different WHSV were applied for some of the samples.

<sup>a</sup>The particles size was determined by XRD.

<sup>b</sup>The particle size was determined by chemisorption.

<sup>c</sup>H<sub>2</sub> co-fed for NiFe (1 : 1) catalyst 80 : 20 ml/min.

<sup>d</sup>Only a few tubes available for study.

main objective is to gain a better understanding of the CNF growth process towards large scale production of CNF for applications in catalysis.

## EXPERIMENTAL

Carbon nanostructures were synthesized by chemical vapour deposition typically in a fixed bed vertical quartz reactor with 4 cm diameter and a length of 50 cm at 600 °C.  $\text{Fe}_3\text{O}_4$  nanoparticles [4], Ni and Fe supported on  $\text{Al}_2\text{O}_3$  prepared by coprecipitation [4–6] and NiFe/ $\text{Al}_2\text{O}_3$  (20 mass %, Ni : Fe ratio is 1 : 1) prepared by deposition–precipitation [7, 8] were used as catalysts. The catalysts were reduced in a hydrogen atmosphere at 600 °C (heating rate 5 °C/min). Reduction was followed by flushing with argon before the reactant mixture was introduced.  $\text{CO}/\text{H}_2$  [4, 6, 7],  $\text{CO}$  [4, 6, 7],  $\text{CH}_4/\text{H}_2$  [4, 5, 8],  $\text{C}_2\text{H}_6/\text{H}_2$  [4] and  $\text{C}_2\text{H}_4/\text{CO}/\text{H}_2$  [6] have been used as gas precursors. The gas compositions are shown in Table 1. The reactor effluent was analyzed by an online GC. Some experiments were also performed at 750 °C, at different partial pressures of reactant, and at different space velocities.

X-ray diffraction (XRD) analysis was carried out to determine catalyst particle size using a Siemens D5000 X-ray diffractometer with  $\text{CuK}\alpha$  radiation. Hydrogen chemisorption was performed with Micrometric ASAP 2000 apparatus with about 0.3 g reduced catalyst samples at 35 °C. Transmission Electron Microscopy was done using a JEOL 2010F electron microscope equipped with a field emission gun.

## RESULTS AND DISCUSSION

Table 1 summarizes the structure, diameter and average growth rate of CNF obtained on different catalysts and different gases. A semi-quantitative comparison is considered although the space velocity is different for some of the experiments. The diameter of the growth catalyst particles is also presented.

The choice of catalyst determines both structural features and carbon yield. The CNF yield is in principle proportional to the metal loading in the growth catalysts, provided that

the metal crystal size is kept constant at different loadings. This is the main reason for selecting hydrotalcite derived catalysts as the CNF growth catalysts in our group, since catalysts with small sized metallic crystals can be achieved with metal loadings as high as 78 mass %. The Ni and Fe catalysts listed in Table 1 were prepared via hydrotalcite precursors. Bimetallic NiFe with different ratios have also been synthesized via hydrotalcite precursors, but only NiFe (1 : 1) prepared by deposition–precipitation method is presented in Table 1. The results clearly indicate that catalyst activity for CNF growth depends significantly on the metal composition. Ni is the most active catalyst for the CNF growth from hydrocarbon while Fe is more active for CNF growth from  $\text{CO}/\text{H}_2$ . It is difficult to directly compare the activity of NiFe catalysts in Table 1 to the Ni and Fe due to different metal loadings. The growth rate of NiFe based on the gram of metal catalyst lies between Fe and Ni catalysts.

A mechanism of CNF growth seems to be generally accepted, where surface reactions lead to formation of surface carbon, dissolution and segregation, diffusion of carbon through bulk metal from the gas-solid side to solid-support side, and precipitation on the support side of the metal particles. The difference in the activity of different metals and alloys might be attributed to the difference in the binding energy of carbon to metals. The binding energy of Ni–C is 41 kJ/mol, and the binding energy of Fe–C is 48 kJ/mol, while the binding energy of NiFe–C lies between Ni and Fe catalysts. The binding energy of Fe–C is relatively high, indicating a strong binding of carbon atoms to the Fe surface. It can also explain why iron carbide can be observed during CNF growth, while no nickel carbide can be observed. The formation of iron carbide seems to decrease the rate of adsorption and surface reactions of methane, and thus the growth rate.

Another important conclusion that can be drawn from Table 1 and Fig. 1 is that the structure of the CNF is determined by the catalyst composition as well as the reactivity of the carbon sources. The effect of the catalyst composition on CNF growth by methane decomposition is clearly demonstrated in Fig. 1. Fishbone CNFs are produced on Ni catalysts

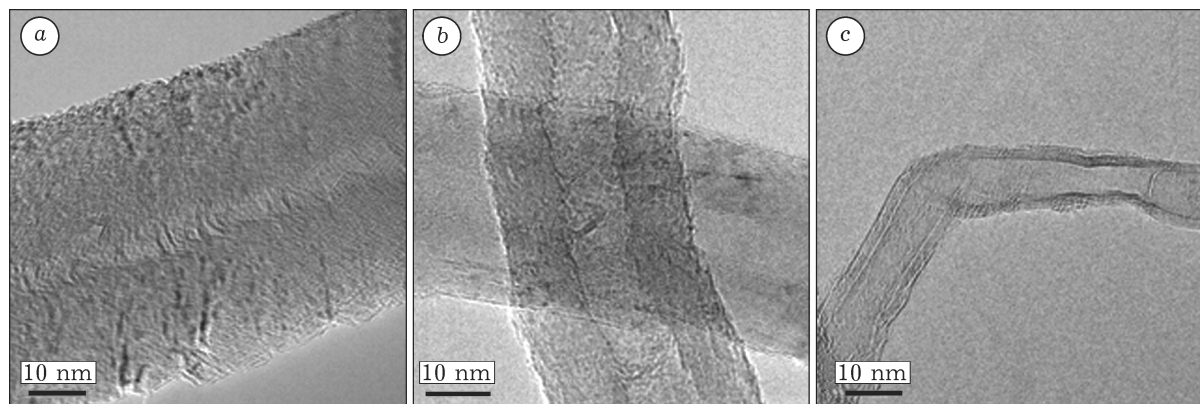


Fig. 1. Carbon nanostructures synthesized from: *a* – Ni (Fishbone); *b* – NiFe (1 : 1) (Fishbone tubular); *c* – Fe (MWNT) using  $\text{CH}_4$  as a catalyst. For NiFe (1 : 1), also  $\text{H}_2$  is present.

and MWCNTs are produced on Fe catalyst. The structure of CNF produced on NiFe alloy catalysts combines the characteristics of the CNF from both Ni and Fe catalysts. It is defined as fishbone-tubular structure (FB-Tubular) in Table 1, while it also has been defined as stacked carbon cup structure [9]. Ni is an active catalyst, and produces mostly fishbone CNF, regardless of the reactivity of the carbon sources. Fe is less active, and the structure of CNF produced depends on the reactivity of the carbon sources. The decomposition of methane and ethane on hydrotalcite derived Fe catalysts mainly yields MWCNTs, while reactions in  $\text{CO}/\text{H}_2$  result mainly in a fishbone like structure with a small inner hole. It seems that the growth rate is a crucial parameter to determine the nanostructures of the synthesized CNFs. Carbon nanotubes can be synthesized by controlling a relatively low growth rate at relatively high temperatures.

Based on this principle, the structure of the MWCNTs can be further controlled by controlling the temperature and the partial pressure of the hydrocarbons. Figure 2 demonstrates that the thickness of the wall of the MWCNTs is reduced when the synthesis conditions of 873 K and 1 bar of ethane are changed to 1023 K and 0.1 bar of ethane on hydrotalcite derived Fe catalysts. In this way, carbon nanotube with few walls (1–5) and with a large inner diameter can be synthesised at lower partial pressure of ethane.

A suitable combination between the catalyst and the carbon source based on the reactivity of the carbon source is important in CNF/CNT

synthesis. The use of a more reactive gas like  $\text{C}_2\text{H}_4$  results in tar or no ordered structures for the supported Fe catalyst, while Ni produces

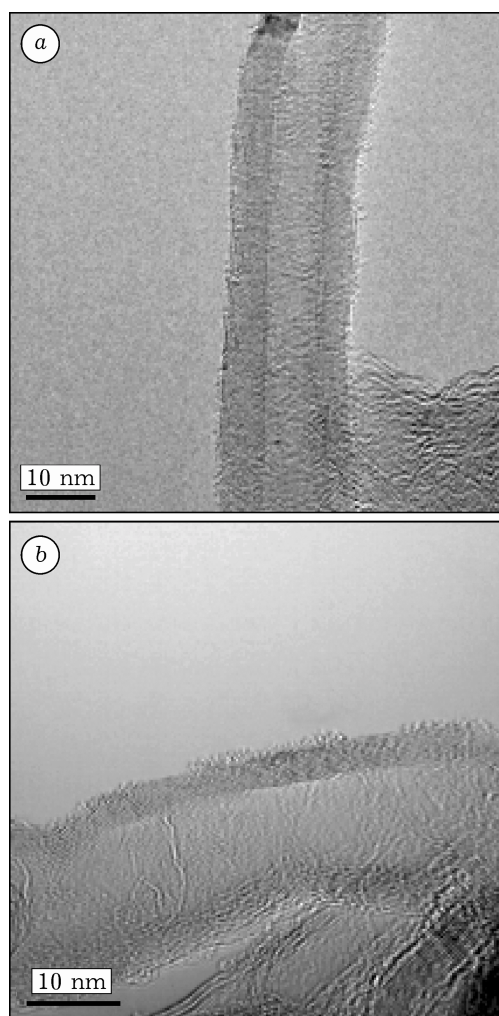


Fig. 2. MWNTs prepared using  $\text{Fe}/\text{Al}_2\text{O}_3$ : *a* – 600 °C,  $p_{\text{C}_2\text{H}_6} = 1$ ; *b* – 750 °C,  $p_{\text{C}_2\text{H}_6} = 0.1$ .

high yields of fishbone CNFs from  $C_2H_4$ . This fishbone structure is, however, of poorer crystallinity than the fishbone prepared from less reactive hydrocarbons. Although higher yields of fishbone can be obtained by changing the gas precursor, there is always a trade off between quality and yield with respect to the application. In general, the CNFs synthesized with a low growth rate have good crystallinity.

Controlling the diameter of CNF is an important issue in the CNF synthesis. It has normally been suggested that control of the CNF/CNT diameter can be obtained by controlling the metal particle size. Our previous work has also demonstrated this principle for CNF synthesis during methane decomposition on different 12 mass % Ni catalysts, where the diameters of CNF are similar to the metal crystal size of the growth catalysts [10]. However, CNFs with diameters larger than the Ni crystal size are obtained on high loading Ni catalysts, as shown in Table 1. Merging of particles to reach a larger and more thermodynamically favourable size for growth has been reported by Ermakova *et al.* [11] for methane decomposition over a Ni catalyst. Moreover, the diameter of the CNFs grown is found to depend significantly on the carbon sources used in the synthesis. The increase in diameter of the structures synthesized for both unsupported and supported Fe for different gases show the same trend:  $CO/H_2 > CO > C_2H_4/CO/H_2 > C_2H_6 > CH_4$ . It is in good agreement with the observation by Toebe [12] that the CNF growth, and thereby the CNF diameter depends on the reactant medium and particle size of the

growth catalyst. It has also been explained in the literature that CNTs are produced only from particles within a certain size range [13, 14].

An alternative explanation on the size dependence on the carbon sources employed in the CNF synthesis is the re-contraction of metal particles induced by dissolved carbon. Experimental and theoretical studies have indicated that carbon dissolved in the metal particles can significantly decrease the melting point of the metal nanoparticles. However, the real state of the metal particles: molten phase or solid phase, is still debated in literature. Observations of the formation of iron carbide and of iron inside the MWCNTs after growth, support the theory of dissolution of carbon in the metal particles [15]. The order of increase in diameter with the carbon sources follows the growth rate of CNF and CNT, expected for the  $C_2H_4/CO/H_2$ . A high growth rate means a high surface reaction rate and thus high site coverage of carbon on the surface, resulting in a high equilibrium concentration of carbon in the metal particles. Molecular dynamic simulations have revealed that dissolution of carbon in spherical iron particles can lead to a spreading action to form a relatively flat shape [16]. Higher concentration of carbon in metals results in a flattening of the metal particle, and thus CNFs of larger diameter.

The use of support as opposed to no support can give very different carbon nanostructures. When using  $CO/H_2$ , unsupported Fe produces platelet CNFs (Fig 3, a), while supported Fe produces the Fishbone-tubular structure (see Fig 3, b). The supported Fe particles have low

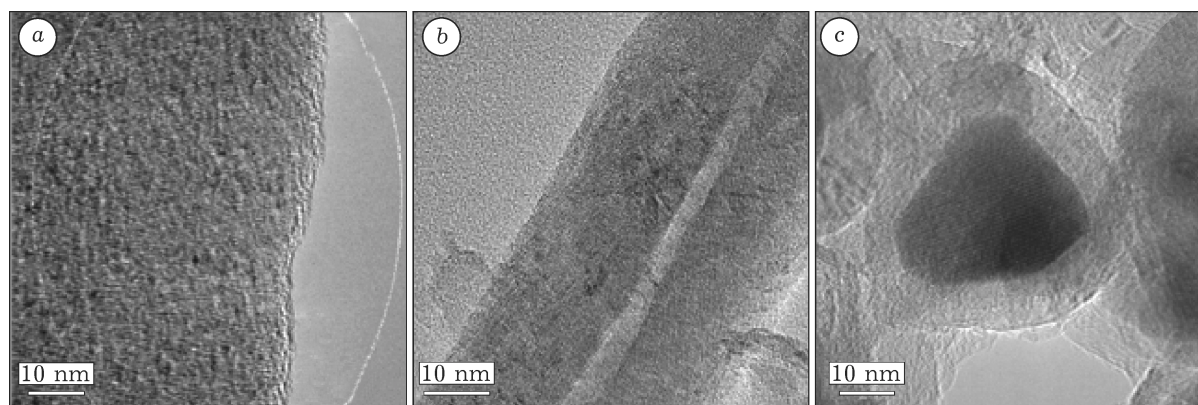


Fig. 3. Carbon nanostructures prepared from  $CO/H_2$ : a – platelet from  $Fe_3O_4$  nanoparticles; b – Fishbone tubular from  $Fe/Al_2O_3$ , from  $CO$ ; c – onion-like carbon nanofibres.

mobility due to the interaction with  $\text{Al}_2\text{O}_3$ , whereas the growth of the unsupported Fe particles is not restricted. The unsupported particles are very mobile due to a large uptake of carbon and are flattened due to a wetting and spreading action which realises growth of platelet carbon nanofibres [17].

The control of hydrogen partial pressure is vital to control the growth from the carbon sources. The results in Table 1 clearly indicate the importance of hydrogen in the nucleation and growth of CNT and CNF on Fe catalysts. In the absence of  $\text{H}_2$ , the Boudouard reaction on Fe catalyst results in a predominantly onion carbon (see Fig 3, c). However, the Boudouard reaction on NiFe catalyst results in mostly MWCNT. Onion carbon has also been observed using pure methane on Fe catalysts. It seems that hydrogen generated from methane decomposition is not enough to prevent the formation of onion carbon. High  $\text{H}_2$  partial pressures were used for the synthesis with  $\text{C}_2\text{H}_6$  which resulted in MWNTs with good quality and crystallinity. It has been suggested that the presence of hydrogen is needed in order to initiate nucleation of CNTs and thereby avoid the formation of onion-like structures [18]. Some tubes are however stacked at a small angle with respect to the fibre axis. This is most likely because  $\text{H}_2$  is able to saturate the dangling bonds of the graphite sheets. [3].  $\text{H}_2$  is also believed to influence the surface orientations of the catalysts by lattice restructuring [3].

Hydrogen has a significant effect on the kinetics of CNF/CNT growth. Surface adsorbed hydrogen helps to avoid the polymerization of adsorbed C species that otherwise will encapsulate and deactivate the catalyst. This effect improves the carbon yield at lower hydrogen partial pressures. At higher partial pressures, the rate of gasification increases and hydrogen suppresses methane adsorption and dissociation. The carbon yield is lowered. Figure 4 shows the effect of space velocity in methane dissociation on the carbon yield. By increasing the space velocity, the hydrogen level is decreased, and the carbon growth rate is increased. The results show that a similar carbon yield that could be synthesized in 30 h (final yield 24.5 g/(g cat. · h)) for the lowest space velocity (see Fig. 4, a) could be obtained in

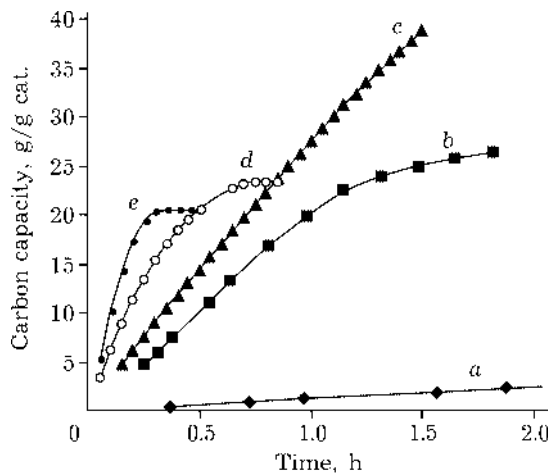


Fig. 4. Carbon capacity as at 600 °C in ceramic horizontal reactor as a function of time for different space velocities of  $\text{CH}_4$ : a – [WHSV: 4.6 l/(g cat. h)], b – [WHSV: 187 l/(g cat. h)], c – [WHSV: 410 l/(g cat. h)] and at 600 °C in vertical quartz reactor: d – [WHSV: 738 l/(g cat. h)], e – [WHSV: 1612 l/(g cat. h)].

around 30 min at higher space velocities (see Fig. 4, d, e). However, higher carbon formation rate results from the higher space velocity, which leads to more polymerization of surface carbon and thereby faster deactivation. There is a trade off between growth rate and carbon capacity to find the suitable conditions.

The results show that a broad focus and detailed knowledge about the catalyst and the operation conditions are needed in order to optimize and develop the synthesis of carbon nanostructures. The optimization lies in choosing the correct combination of catalyst system (activity), reactant mixture (reactivity) and temperature, together with good control of hydrogen partial pressure. The space velocity or partial pressure of hydrogen in the reactor seems to be the most important parameter in scale-up of the reactor for CNT/CNF synthesis.

## CONCLUSION

The results summarized in this communication reflect the complex nature of CNF synthesis by chemical vapour deposition. The synthesis of large amounts of preferred carbon nanostructure relies on careful control of the operating conditions and catalyst system. Control of  $\text{H}_2$  partial pressure, reactant partial pressure and temperature is important, but the

opportunities which lie in the modification of the catalyst system are equally interesting. Ni and Fe typically produce fishbone and MWNTs, respectively. Using the bimetallic NiFe catalyst can yield structures intermediate to the two individual metal catalysts. If the yield is improved it can be an exciting candidate for applications where the MWNT properties together with the availability of graphite edges are important.

## REFERENCES

- 1 K. P. de Jong and J. W. Geus, *Catalysis Rev.: Sci. and Eng.*, 42 (2000) 481.
- 2 C. Park and R. T. K. Baker, *J. Phys. Chem. B*, 102 (1998) 5168.
- 3 P. E. Nolan, M. J. Schabel and D. C. Lynch, *Carbon*, 33 (1995) 79.
- 4 Z. Yu, D. Chen, B. Totdal and A. Holmen, *J. Phys. Chem. B*, 109 (2005) 6096.
- 5 I. Kvande, Z. Yu, M. Rønning *et al.*, to be submitted.
- 6 Z. Yu, B. Totdal, M. Rønning *et al.*, to be submitted.
- 7 Z. Yu, D. Chen, B. Totdal *et al.*, *Appl. Catal., A: Gen.*, 279 (2005) 223.
- 8 T. Zhao, PhD dissertation, UNILAB, State Key Laboratory of Chemical Reaction Engineering, East China University of Science and Technology, 2004.
- 9 M. Endo, Y. A. Kim, T. Hayashi *et al.*, *Appl. Phys. Lett.*, 80 (2002) 1267.
- 10 D. Chen, K. O. Christensen, E. Ochoa-Fernandez *et al.*, *J. Catal.*, 229 (2005) 82.
- 11 M. A. Ermakova, D. Y. Ermakov, L. M. Plyasova and G. G. Kuvshinov, *Catal. Lett.*, 62 (1999) 93.
- 12 M. L. Toebes, J. H. Bitter, A. J. van Dillen and K. P. de Jong, *Catal. Today*, 76 (2002) 33.
- 13 H. Dai, A. G. Rinzler, P. Nikolaev *et al.*, *Chem. Phys. Lett.*, 260 (1996) 471.
- 14 O. A. Nerushev, S. Dittmar, R. E. Morjan *et al.*, *J. Appl. Phys.*, 93 (2003) 4185.
- 15 M. A. Ermakova, D. Y. Ermakov, A. L. Chuvilin and G. G. Kuvshinov, *J. Catal.*, 201 (2001) 183.
- 16 F. Ding, A. Rosen and K. Bolton, *Phys. Rev. B: Condensed Matter and Mat. Phys.*, 70 (2004) 075416/1.
- 17 R. T. K. Baker, J. J. Chludzinski, Jr. and R. D. Sherwood, *Carbon*, 23 (1985) 245.
- 18 L. Dong, J. Jiao, S. Foxley *et al.*, *J. Nanoscience and Nanotechnol.*, 2 (2002) 155.